Arch. Metall. Mater. **62** (2017), 1, 437-444

DOI: 10.1515/amm-2017-0066

G. WLOCH*#, T. SKRZEKUT*, J. SOBOTA**, A. WOZNICKI*, L. BŁAŻ*

SILVER MATRIX COMPOSITE REINFORCED BY ALUMINIUM-SILVER INTERMETALLIC PHASES

Silver and aluminum powders (82 mass % Ag and 18 mass % Al) were mixed and hot extruded at 673 K with extrusion ratio $\lambda = 25$. Performed X-ray diffraction analysis of as extruded rod revealed the development of Ag_3Al and Ag_2Al-type intermetallic phases. Structural observations and both chemical and diffraction analysis of structural components confirmed the growth of mentioned phases in the vicinity of elementary Al and Ag granules. No pores or voids were observed in the material. Mechanical properties of the composite, UTS = 490MPa, YS = 440 MPa, HV2 = 136, were relatively high if compared to commercial Ag and Cu products. Hot compression tests pointed to the good hot workability of the composite at deformation temperature range 473 K – 773 K.

The differential scanning calorimetry tests were performed in order to estimate structural processes during heating of Ag/Al composite that lead to thermodynamically stable liquid state. It was found that characteristic temperature of three endothermic peaks correspond to (1) peritectoid transformation μ-$Ag_3Al \rightarrow \zeta$-Ag_2Al + (Ag), (2) the eutectic melting ζ-Ag_2Al + (Al) → L, (3) melting of the ζ-Ag_2Al phase.

The Vickers hardness of the samples annealed at 673 K, for the time range up to 6900 minutes, was also determined. It was concluded that mutual diffusion of elements between Ag and Al granules and the growth of μ-Ag_3Al and ζ-Ag_2Al grains during annealing at 673 K result in a slight hardening of the composite.

Keywords: Silver-aluminum composite, powder metallurgy, plastic consolidation, Ag-Al intermetallics

1. Introduction

High conductivity is a principal attribute of silver, aluminum, and copper based materials and often become preselected as a leading parameter of materials used in electronic devices and electric power equipment. However, relatively low mechanical properties of the pure metals raise a challenge for metallurgy engineers, who are searching for new high-strength materials having good electrical properties. The most common methods of the material strengthening are based on strain hardening or appropriate alloying and precipitation hardening of alloys. However, both increased dislocation density as well as increased content of alloying elements in solid solution reduces required conductivity parameters. Therefore, the development of new materials for mentioned demands have to start from careful selection of alloying components as well as an application of appropriate mechanical processing route and heat treatment conditions.

As mentioned formerly, an increased content of alloying elements in solid solution reduces the conductivity [1]. Therefore, the most awaited effects, i.e. the material strengthening and high conductivity, can be achieved due to structural processes that combine the precipitation hardening and efficient reduction of solutes in the matrix during the heat treatment of the alloy [1-4].

During last decades particular attention was paid to the production of sheets and wires made from copper-silver alloys containing up to 15 mass% Ag [5-11]. Initial grains of hypoeutectic or eutectic Cu-Ag alloy are elongated during drawing with high reduction ratio that leads to the formation of quasi-composite structure of the wire containing very thin Ag-type fibers in Cu-matrix. Grain coarsening during annealing of heavy deformed wires is practically limited to the distance between Cu/Ag interfaces. In consequence, the average grain size in as-annealed material decreases with the reduction of the wire diameter that increase the strength of the material up to UTS = 1000 – 1300 MPa [10,11]. It is worth stressing that the conductivity of the composites becomes lower than that for pure copper (65%IACS – 80%IACS) [10].

The most effective strengthening of Al, Cu, Ag-based materials was reported for mechanically alloyed (MA) composites reinforced with fine metal-oxide particles [12-20]. However, both costly and time-consuming processing of the materials and low efficiency of used procedures put the meaningful limitation for the application of MA composites in practice. Moreover, chemical reactivity of constituents and increased diffusivity of elements at high enough temperature lead to the transformation of structural components that usually results in the reduction of strength and increasing porosity of the composite.

* AGH – UNIVERSITY OF SCIENCE AND TECHNOLOGY IN CRACOW, FACULTY OF NON-FERROUS METALS, AL. A. MICKIEWICZA 30, 30-059 KRAKÓW, POLAND
** STATE HIGHER VOCATIONAL SCHOOL IN TARNOW, POLYTECHNIC INSTITUTE, DEPARTMENT OF MATERIALS ENGINEERING

Corresponding author: gwloch@agh.edu.pl

Highly refined structure of metallic materials can also be achieved due to cyclic extrusion/compression (CEC) procedure [21-22], however, CEC is not practically usable method for the large-scale production.

Relatively efficient powder metallurgy and sintering methods were also applied for manufacturing composites, which show high arc resistance. Effects of zinc oxide (ZnO), silver tungstate (Ag_2WO_4) and silver molybdate (Ag_2MoO_4) additions on sintered Ag-based electric contacts were tested [18]. However, the metal-oxide strengthening of considered low-resistant metals should always be carefully considered with respect to expected chemical reaction at high temperatures and related arc resistance of the composite.

Highly advanced method for manufacturing of Cu-based composite reinforced with Nb-fiber was presented by Rdzawski et al. [23-24]. High strength Cu-based composite wires reinforced with Nb-filaments were developed for specific practical applications such as the winding of generators producing strong and variable magnetic fields. Multi-fiber Cu-Nb composite wires were produced by means of multistage drawing of bundled Cu-coated niobium wires. Due to multiple folding of as-drawn composite wires, more than 820,000 niobium filaments uniformly distributed in Cu-matrix, having 100 nm-200 nm in diameter, were received [23-24]. Tensile strength of 900-1120 MPa and electrical conductivity of 40-45 MS/m were attained.

Literature search for high-strength composites having comparable resistivity to mentioned formerly group of metals (Cu, Ag, Al), lead to the conclusion that there is a lack of data for Al-Ag composites produced by means of mechanical consolidation of silver and aluminum powders. Therefore, experiments described below were undertaken to test practical aspects of mechanical coupling of Al and Ag powders by means of pressing and hot extrusion methods. It was assumed that expected structural combination of aluminum/silver grains is not available if any metallurgical methods are used because of a few phase-transformation reactions in Ag-Al system and one or two intermetallic phases development in as-cast Ag-alloys containing above ~5 wt.% aluminum addition.

2. Experimental work

Silver and aluminum powders having particles size ≤63 μm and purity of 99.96% Ag and 99.7% Al, respectively, were used for manufacturing a bulk Ag/Al composite. The powder mixture, containing 81.9 mass % (53.1 at %) Ag and 18.1 mass % (46.9 at. %) Al, was preliminarily mixed using TURBULA T2F mixer and consolidated by compression at the room temperature using 500 kN press. As obtained billet, 40 mm in diameter and ~60 mm long, was hot extruded at 673 K and rod of 8 mm in diameter was received (extrusion ratio: $\lambda = 25$).

Mechanical properties of as extruded rods were tested using Zwick/Roell Z050 tensile testing machine equipped with extensometers that provided precise determination of the sample elongation, Young modulus and Poisson ratio. Hardness tests were performed using Vickers method and Shimadzu HMV hardness tester. An indenter load of 19.61N and dwell time 10 s were used. Annealing tests at 673 K in a range up to 6900 minutes were performed in order to test the effect of annealing time on hardness and structure of the material.

Effectiveness of mechanical consolidation of Ag/Al powders was also considered on the basis of density measurements. Density of as extruded material was determined by Archimedes method.

Resistivity of as extruded rod was tested by means of four-point probe method and Thompson-Kelvin BURSTER RESISTOMAT 2304 bridge device. The measurements were performed at 294.8 K for samples 150 mm in length and 6,6 mm in diameter.

Structural observations were performed using a light microscope Nikon Epiphot 200 and a scanning electron microscope Hitachi SU 70 equipped with EDS detector and STEM system. Additional microstructure analyses were performed by means of transmission analytical electron microscope JEM2010. Samples for light microscopy and SEM observations were mechanically grinded with abrasive paper and polished using diamond suspension. Thin foils for the STEM/TEM observations were mechanically grinded and discs ∅ = 3 mm and ~0.04 mm in thickness were finally thinned by means of Gatan PIPS 691 ion thinning machine.

Phase analysis of the material was performed with X-ray Rigaku MiniFlex II diffractometer. The sample was mechanically powdered and fixed to the holder of the diffractometer.

Complementary tests concerning phase transformation analyses during heating of the composite samples were based on differential scanning calorimetry (DSC). DSC tests were performed at a temperature range 293-973 K using Mettler Toledo DSC 821e calorimeter and heating rate of 20 K/min.

3. Results

Mechanical and physical properties

Selected mechanical and physical properties of as extruded Ag-Al composite, tested at 293 K, are presented in Table 1. Effect of annealing at 673 K on the composite hardness is shown in Fig. 1. It was found that the material hardness rose from HV = 136 to HV = 151 for as extruded material and a sample annealed at 673 K/115 h, respectively.

Flow stress characteristics at 293 K – 773 K were tested by means of hot compression test at constant true strain rate of 10^{-3} s^{-1} (Fig 2). The flow curves $\sigma_t - \varepsilon_t$ observed at high temperature range are typical for Al-based materials undergoing intense dynamic recovery during deformation [25]. The samples deformed at 473 K – 773 K did not fracture within the deformation range used in the compression test (max. $\varepsilon_t \approx 0.4$). However, samples deformed at relatively low temperature have fractured during compression. The effect of deformation temperature on the flow stress maximum is shown in Fig. 2b. Open marks at 293 K – 373 K are used to stress the fact that static flow regime was not attained during deformation and the sample has fractured before the end of testing.

TABLE 1

Mechanical and physical properties of as extruded Ag-Al composite

Ultimate tensile strength, R_m	490 MPa
Yield stress, $R_{p0.2}$	440 MPa
Elongation, A	5 %
Young modulus, E	80 GPa
Poisson ratio, ν	0,3
Hardness, HV2	136
Electrical resistivity, ρ	90,2 nΩm
Density, d	6,8 g/cm^3

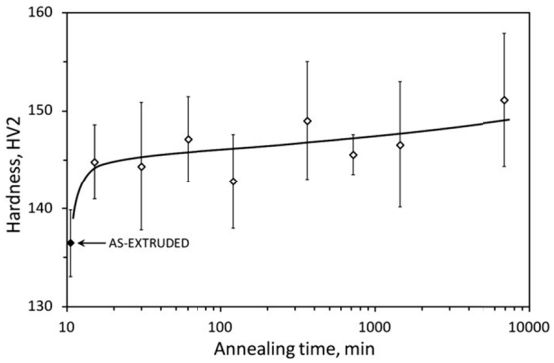

Fig. 1. Effect of annealing at 673 K on Ag-Al composite hardness

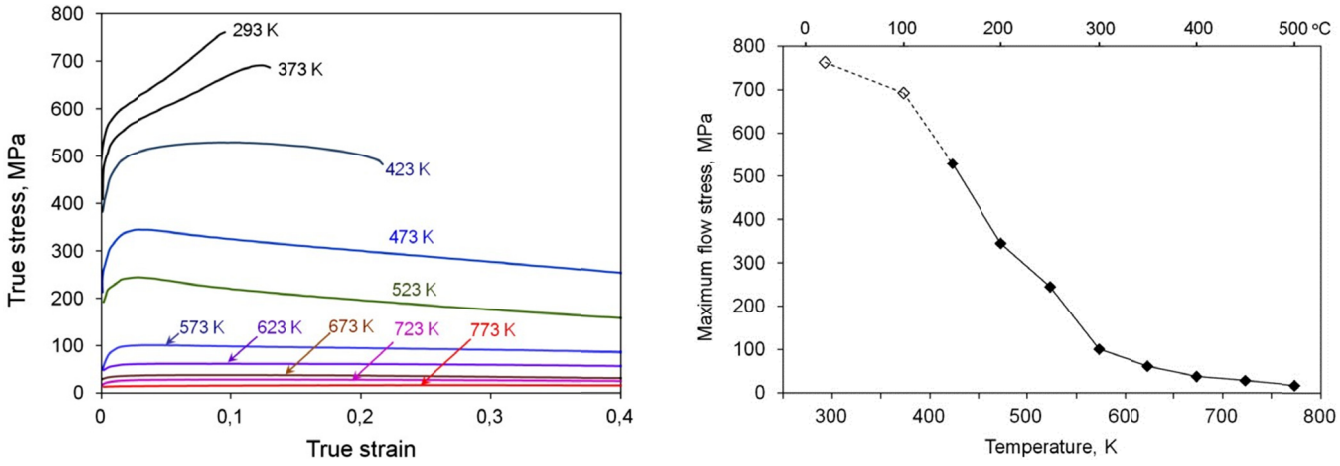

(a) (b)

Fig. 2. Effect of deformation temperature on the flow stress characteristics observed for as extruded Ag/Al alloy: (a) $\sigma_t - \varepsilon_t$ curves observed at deformation temperature marked in the figure; (b) effect of deformation temperature on the flow stress maximum detected during compression test

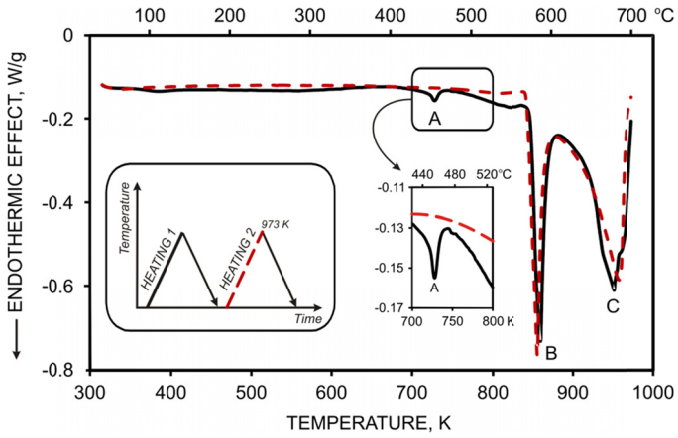

Fig. 3. DSC curves received for as extruded Ag/Al composite ("heating 1" – solid line) and obtained during repeated heating of the sample ("heating 2" – dashed line). Scheme of heating/cooling procedure and vertically expanded graph for A-effect are inserted in the figure

It is worth to notice that structural processes during annealing or hot compression tests were diffusion controlled at solid state conditions. Therefore, complementary DSC tests were performed in temperature range 293 K – 973 K in order to test both diffusion controlled effects at solid state as well as the effect of fastened diffusion on transformation processes in semi-liquid material. DSC curve, recorded during heating of as extruded sample at 293 K – 973 K (heating rate 20°C/min) revealed three endothermic effects are marked A, B and C in the Fig. 3. The peak A is not observed on DSC curve if already tested sample is heated again at the same heating/cooling rate of 20 K/min (dotted line).

Structural observations

Morphology of the elementary silver and aluminum powders is shown in Fig. 4. The powder granules were found to form agglomerates, which were irregular in shape and larger than formerly mentioned value of 63 mm. Therefore, prolonged mixing of the powders was necessary for braking agglomerates and receiving relatively homogeneous distribution of components after mechanical consolidation of powders. Structural observations of as extruded rods revealed practically uniform distribution of the composite components (Fig. 5). Both silver and aluminium granules were elongated in the extrusion direction and no pores or cavities were found. The result evidences a good powder particles consolidation during the manufacturing process.

However, hot extrusion conditions are not convenient for maintaining initially pure Al/Ag components and intermetallic

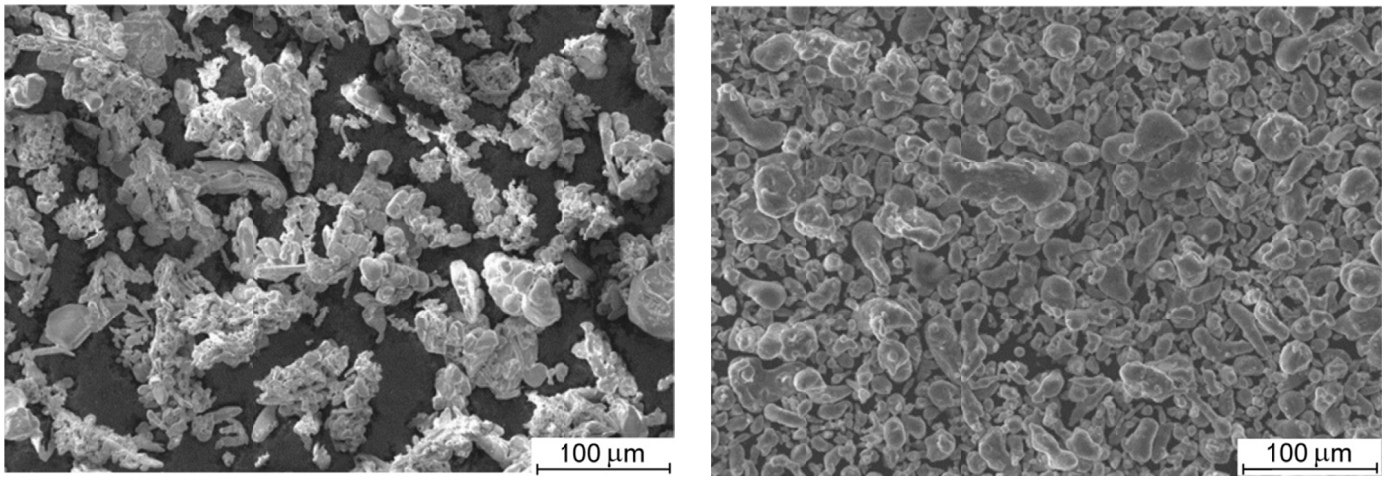

(a) (b)

Fig. 4. Morphology of the elementary powders (SEM): a) Ag, b) Al

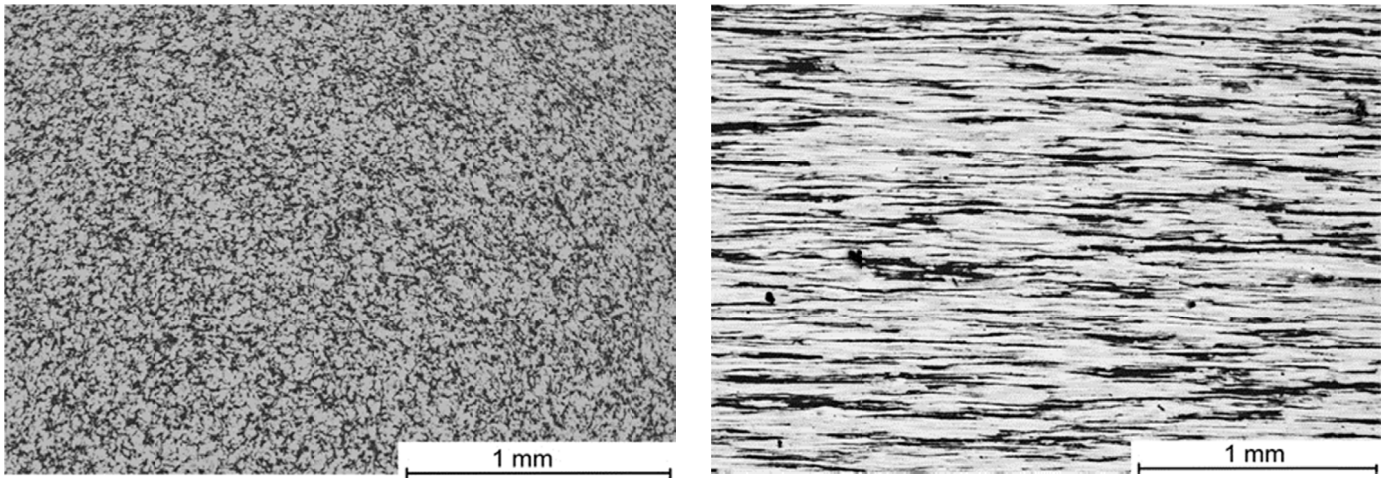

(a) (b)

Fig. 5. SEM microstructure of as extruded Ag/Al composite: a) cross-sectioned rod; b) longitudinally sectioned rod

components growth cannot be avoided. XRD analysis of as extruded material revealed characteristic peaks for Ag, Al as well as Ag_3Al and Ag_2Al phases as shown in Fig. 6.

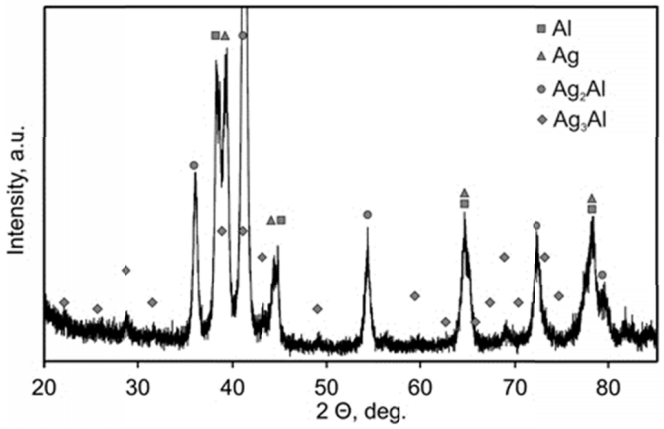

Fig. 6. XRD phase analysis of as-extruded material

Structural observations performed by means of STEM/EDS element mapping revealed specific distribution of elements as shown in Fig. 7. Apart from Ag and Al grains, additional structural components containing the two elements were observed in the vicinity of Ag/Al boundaries. Detailed analysis of mentioned area was performed at relatively high magnification as shown in Fig. 8. Chemical composition of characteristic structural components, which differed in the gray threshold, were tested using EDS analysis. The results are presented in Table 2.

Transmission electron microscopy observations and SAD pattern analysis confirmed the development of intermetallic grain structures in the vicinity of initially pure Ag and Al components. For example, the development of Ag_2Al (grain B) in the vicinity of initial Al-granules (A, D) was shown in Fig. 9. The stoichiometry of Ag_2Al is confirmed by EDS analysis (Tab. 3) and inserted SAD pattern corresponds to the crystallographic structure Ag_2Al, hcp (disordered), a = 0.2878 nm, c = 0.4625 nm [26].

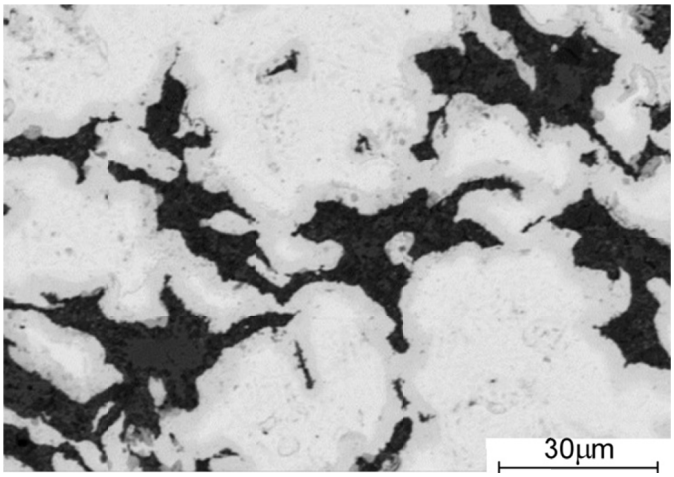

(a)

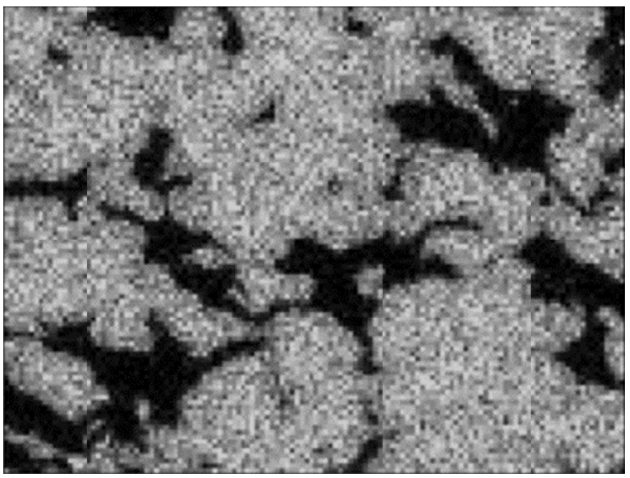

(b)

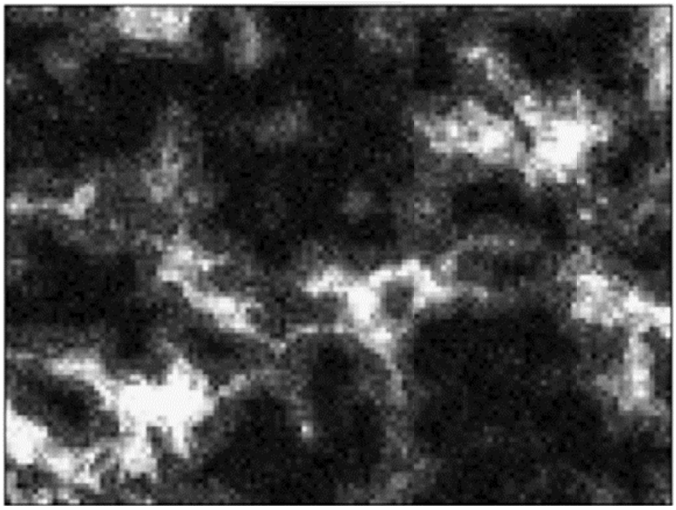

(c)

Fig. 7. Element mapping results for cross-sectioned as extruded Ag/Al composite rod

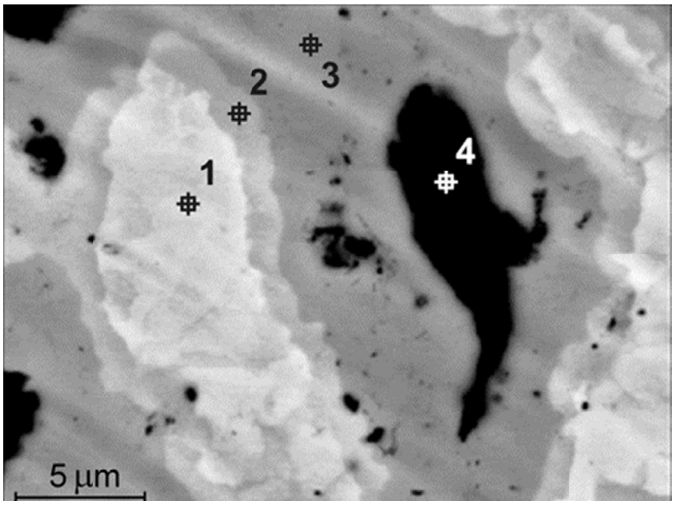

Fig. 8. SEM/EDS microanalysis of structural components in as extruded Ag/Al composite (Results are presented in Table 2)

TABLE 2

Chemical composition detected by EDS for selected grains marked in Fig. 8

Grain	Ag at.%	Al at.%
1	96.2	3.8
2	78.1	21.9
3	63.0	37.0
4	8.5	91.5

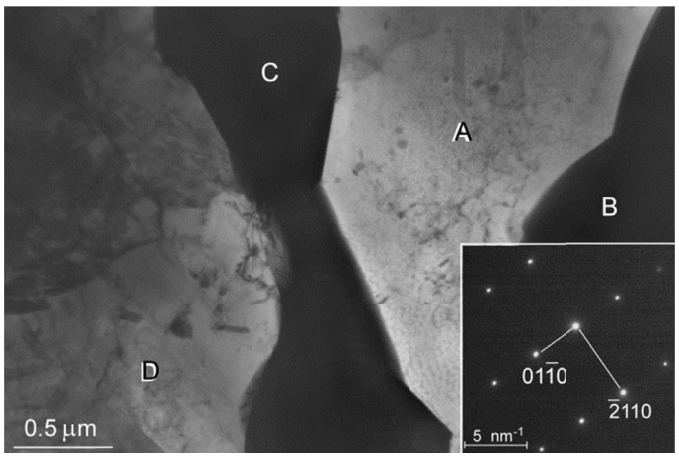

Fig. 9. TEM microstructure of as extruded Ag/Al rod; EDS analysis results for grains A, B, C, D are shown in Table 3. SAD pattern confirms Ag_2Al structure of the B-grain (see: inset)

TABLE 3

EDS analysis results for grains marked A, B, C, D in Fig. 9

Grain	Al	Ag
A	96.0	4.0
B	33.8	66.2
C	32.5	67.5
D	98.5	1.50

All results in atomic%

4. Discussion

Hot extrusion resulted in effective consolidation of elemental Ag and Al powder granules and receiving fine-grained structure of the composite (Fig. 5). Mechanical properties of as extruded Ag/Al composite are relatively high (Tab. 1) with respect to commercial aluminum or silver products. The addition of 18 mass % Al leads to considerable reduction of the composite density that is often desired in practical applications. However, diffusion and reaction of one element to another in the vicinity of elementary Ag/Al boundaries, which take place during extrusion at 673 K, were found to result in the growth of two intermetallic layers dividing original Al/Ag grains (Fig. 6-9). Diffusion of Ag and Al elements into neighboring elementary granules was efficient enough to form solid solutions (Ag) and (Al) as well as to cause Ag_2Al and Ag_3Al type phases development. It is an obvious statement that Ag_2Al phase should be formed in the vicinity of (Al) grains and Ag_3Al should grow near (Ag) granules that was confirmed by STEM and TEM observations (Fig. 8, Fig. 9). Such effects can be expected if thermodynamically stable Al-Ag diagram (Fig. 10) is taken into consideration. The thickness of Ag_2Al-type coating around Al-grain (marked "3" in Fig. 8) is evidently larger than that for Ag_3Al (marked "2"). Apart from the annealing time/temperature conditions, the thickness of ζ-Ag_2Al and μ-Ag_3Al layers mostly depends on the diffusional constants for the elements in particular phases as well as the concentration gradient i.e. the specific composition of neighboring grains of solid solutions and intermetallic compounds [27-29]. The growth kinetics for particular phases depends also on the driving force of the reaction i.e. specific enthalpy of particular phase formation. Relatively wide composition range of ζ-Ag_2Al phase development (Fig. 10) may also be assumed to contribute to the phase layer thickening with respect to relatively narrow μ-Ag_3Al layer. Therefore, a simple explanation for different thickness of mentioned intermetallic layers needs further studies. Mutual diffusion Ag $\rightleftarrows$ Al leads to both (Ag) and (Al) solutions development and following growth of intermetallic components of the Ag/Al composite structure. In consequence, relatively high electrical resistivity of 90,2 n$\Omega \cdot$m is received that significantly exceeds the value of 21.6 n$\Omega \cdot$m, which is an averaged resistivity for a simple mixture of elemental Ag:Al granules having a volume ratio of 1:0.853.

Annealing at 673 K was found to result in the composite hardness increase from HV136 to HV150 for as extruded material and the sample annealed for 115 h, respectively (Fig. 1). The hardening effect was ascribed to the progress of the initial Ag/Al granule's replacement by relatively hard intermetallic grains.

It is obvious statement that the structure of as extruded composite does not correspond to the phase composition of thermodynamically stable Ag-Al alloy. Structure transformation at solid state is diffusion controlled and depends on annealing temperature. It is assumed that Ag/Al composite material shall finally reach a thermodynamically stable state if an intensive diffusion of elements proceeds at the liquid or semiliquid state. Therefore, DSC experiments were performed at the temperature range 293 K – 973 K that cover the melting temperature for Al-granules and pre-existing ζ-Ag_2Al grains. Remaining unmolten Ag granules can dissolve more intensively in a liquid solution with respect to relatively slow diffusion controlled processes at solid state conditions. DSC results shown in Fig. 3 can be discussed with respect to the phase diagram (Fig. 10). The average composition of Ag/Al composite is marked using dotted line on the diagram. Three endothermic effects, which were revealed on DSC curve for as extruded material, are marked A, B, C on Fig. 3. The first, small peak (marked with A) appears at the temperature ~728 K that corresponds to peritectoid transformation [30]:

$$\mu\text{-}Ag_3Al \rightarrow (Ag) + \zeta\text{-}Ag_2Al$$

Although the average composition of as extruded composite is far out of the range of this transformation, the presence of the μ-Ag_3Al phase in the material microstructure was found (Fig. 6, Fig. 8). If already tested sample is heated again according to the same heating/cooling scheme, the A-peak is not observed on DSC

curve (see: dotted line in Fig. 3). The vanishing of the peak A results from completed diffusion reaction between components at semi-liquid mixture of the composite components at 973 K. So, the peak 'A' for as extruded composite can be ascribed to the decomposition of the μ-Ag_3Al phase to the (Ag) and the ζ-Ag_2Al phase.

The next endothermic peak 'B', observed at ~839 K, corresponds to the eutectic melting:

$$\zeta\text{-}Ag_2Al + (Al) \rightarrow L$$

The following spread peak 'C' results from the melting of the ζ-Ag_2Al grains within the temperature range of 839 K – 943 K.

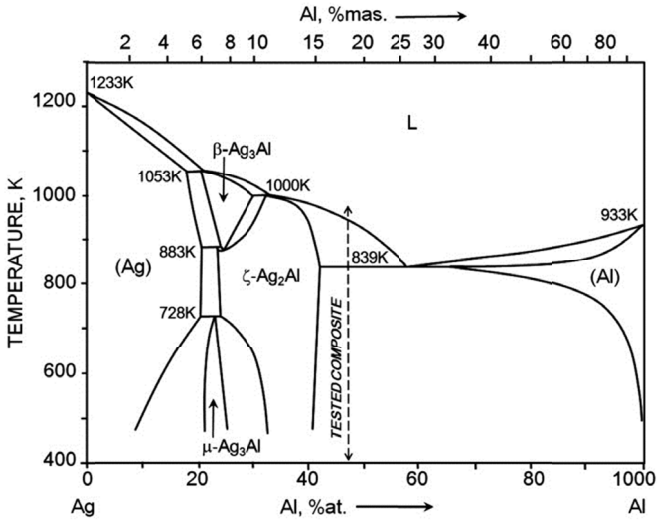

Fig 10. Phase equilibrium Ag-Al diagram drawn according to [30]. The average composition of tested Ag/Al composite is marked in the figure (dotted line)

The XRD phase analysis (Fig. 6) confirmed the presence of described above phases in the as extruded material. However, characteristic peaks corresponding to μ-Ag_3Al phase were scarcely observed. For that reason, additional detailed microstructure investigations using STEM were performed. Careful SEM/EDX and TEM observations revealed two transitional regions between (Ag) and (Al) solid solutions (marked '2' and '3' in Fig. 8). The chemical composition of specific grey layers '2' and '3' tested by EDS corresponds to μ-Ag_3Al and ζ-Ag_2Al phase composition, respectively. TEM observations and SAD pattern analysis also confirm the development of ζ-Ag_2Al grain that has formed in the vicinity of (Al)-granule.

5. Conclusions

Using compression of mixed aluminum and silver powders and following hot extrusion methods, a well-consolidated silver-aluminium composite can be produced. The material porosity is negligible. No pores were found during the microstructure observation.

Mutual diffusion of Al/Ag elements during hot extrusion at 673 K results in the initialization of the phase transformation processes. The microstructure analysis of as extruded composite, including SEM/EDS, TEM/EDS/SAD observations, revealed two layers of μ-Ag_3Al and ζ-Ag_2Al type cover surrounding elementary Al and Ag granules.

The development of intermetallic phases and a local enrichment of Ag(Al) and Al(Ag) solid solution layers result in strengthening of the composite (UTS = 490MPa, YS = 440 MPa, HV = 136). Moreover, the annealing of the material at 673 K causes further increase in the material hardness ascribed to the growing effect of Ag⇄Al diffusion and related local phase transformation effects.

Electrical resistivity of as extruded composite (ρ = 90,2 n$\Omega\cdot$m) is higher than the value expected for a simple mixture of Al and Ag granules (ρ = 21.6 n$\Omega\cdot$m). Relatively high resistivity of the material results from the mutual diffusion of Ag⇄Al elements leading to the enrichment of the primary Ag and Al granules surface layers with the neighbouring element and intermetallic grains growth.

Melting of as extruded Ag/Al composite during heating to 973 K at 20 K/s results in enhanced diffusion of elements between solid Ag-type remnants and a Ag-Al liquid solution. DSC characteristics confirmed the diffusion controlled phase transformations that finally lead to the thermodynamically stable Ag/Al system after one heating/cooling cycle.

Acknowledgements

The authors are grateful to D.Sc. Andrzej Mamala from AGH-University of Science and Technology, Faculty of Non-Ferrous Metals for his help in the experimental work. Financial support from the National Science Centre grant No.: 2011/01/B/ST8/03012 is kindly acknowledged.

REFERENCES

[1] S.O. Kasap, Principles of electrical engineering materials and devices, 2000 McGraw-Hill, Boston.
[2] A. Korbel, W. Bochniak, A. Pawełek, Archiwum Hutnictwa **26**, 253-275 (1981).
[3] S. Karabay, Mater. Design 29 (7), 1364-1375 (2008).
[4] T. Knych, M. Piwowarska-Uliasz, P. Uliasz, Arch. Metall. Mater. **59** (1), 339-343 (2014).
[5] Y. Sakai, K. Inoue, H. Maeda, Acta Metall. Mater. **43**, (4), 1517-1522 (1995).
[6] M.S. Lim, J.S. Song, S.I. Hong, J. Mater. Sci. **35** (18), 4557-4561 (2000).
[7] S. Nestorovic, I. Markovic, D. Markovic, Mater. Design **31** (3), 1644-1649 (2010).
[8] Y.Z. Tian, Z.F. Zhang, Mat. Sci. Eng. A-Struct. **508** (1-2), 209-213 (2009).
[9] J.B. Liu, L. Meng, Y.W. Zeng, Mat. Sci. Eng A-Struct. **435-436**, 237-244 (2006).

[10] A. Kawecki, T. Knych, E. Sieja-Smaga, A. Mamala, P. Kwaśniewski, G. Kiesiewicz, B. Smyrak, A. Pacewicz, Arch. Metall. Mater. **57** (4), 339-343 (2012).
[11] Y. Sakai, K. Inoue, T. Asano, IEEE T. Magn. **28** (l), 888-891(1992).
[12] L. Błaż, J. Kaneko, M. Sugamata, Mater. Chem. Phys. **81** (2-3), 387-389 (2003).
[13] T. Skrzekut, A. Kula, L. Błaż, G. Włoch, M. Sugamata, Int. J. Mater. Res. **105** (3), 282-287 (2014)
[14] A. Kula, L. Błaż, J .Kaneko, M. Sugamata, Journal of Microscopy **237** (3), 421–426 (2010).
[15] L. Blaz, Z. Sierpinski, M. Tumidajewicz, J. Kaneko and M. Sugamata, Mater. Sci. Tech. Ser. **20** (12), 1639-1644 (2004).
[16] G.R. Khayati, K. Janghorban, Adv. Powder Technol. 23 (6), 808–813 (2012)
[17] U. Grundmann, M. Gerner, M. Heilmaier, U. Martin, L. Schultz, H. Oettel, Mater. Sci. Eng. A-Struct. 234-236, 505-508 (1997)
[18] B. Juszczyk, J. Kulasa, A. Gubernat, W. Malec, L. Ciura, M. Malara, L. Wierzbicki, J. Golebiewska-Kurzawska, Arch. Metall. Mater. **57** (4),1063-1073 (2012).
[19] C.P. Wu, D.Q. Yi, J. Li, L.R. Xiao, B. Wang, F. Zheng, J. Alloy. Compd. **457** (1-2), 565-570 (2008).
[20] M. Braunovic, N. K. Myshkin, V. V. Konchits, Electrical Contacts: Fundamentals, Applications and Technology, 2006 CRC Press.
[21] M. Richert, J. Richert, A. Hotloś, P. Pałka, W. Pachla, M. Perek, Mater. Sci. Forum **667-669**, 145-150 (2011)
[22] M.W. Richert, J. Richert, A. Hotlos, M. Mroczkowski, T. Tokarski, Arch. Metall. Mater. **58** (1), 73-75 (2013).
[23] W. Głuchowski, J.P. Stobrawa, Z.M. Rdzawski, K. Marszowski, Journal of Achievements in Materials and Manufacturing Engineering **46** (1), 40-49 (2011).
[24] Z. Rdzawski, W. Głuchowski, J. Stobrawa, W. Kempiński, B. Andrzejewski, Arch. Civ. Mech. Eng. **15** (3), 689-697 (2015).
[25] H. McQueen, S. Spigarelli, M.E. Kassner, E. Evangelista, Hot Deformation and Processing of Aluminium Alloys, 2011 CRC Press
[26] Data from the software of X-ray Rigaku MiniFlex II diffractometer cited according to J.P. Neumann, Y.A. Chang, T. Metall. Soc. AIME **242**, 700 (1968).
[27] V.I. Dybkov, J. Phys. Chem. Solids **47** (8), 735-740 (1986).
[28] V.I. Dybkov, J. Mater. Sci. **21** (9), 3078-3084 (1986).
[29] V.I. Dybkov, J. Mater. Sci. **21** (9), 3085-3090 (1986).
[30] B. Predel, Phase Equilibria, Crystallographic and Thermodynamic Data of Binary Alloys, 1998 Springer, Berlin.